



Kinetics of extracting magnesium by reduction of prefabricated pellets with silicon–calcium alloy powder under relative vacuum

Jun-hua GUO, Ting-an ZHANG, Ji-biao HAN, Yao-song WANG

Key Laboratory of Ecological Metallurgy of Multimetal Intergrown Ores of Ministry of Education,
School of Metallurgy, Northeastern University, Shenyang 110819, China

Received 10 November 2021; accepted 18 April 2022

Abstract: The extraction of magnesium by prefabricated pellets with CaSi_2 as reductant was studied under relative vacuum. The morphologies, chemical compositions and phases of the reduction slag were analyzed using scanning electronic microscopy (SEM), energy dispersive spectrometry (EDS), and X-ray diffraction (XRD), respectively. The results showed that a small amount of argon flow could greatly improve the reduction rate of MgO . The process of extracting magnesium from prefabricated pellets under relative vacuum could be well explained by Model F_1 . The process of reducing magnesium oxide by CaSi_2 was a solid–liquid reaction. This process was controlled by chemical reaction, the temperature had a great influence on the reduction reaction, and the value of the apparent activation energy was 108.99 kJ/mol. The phase analysis of reduction slag showed that the content of MgO had an effect on the crystal transformation of Ca_2SiO_4 .

Key words: isothermal kinetics; magnesium; calcium disilicide; flowing argon; silicothermic process

1 Introduction

Magnesium is one of the most common metals in structural materials. It is also the lowest density metal in engineering materials. As a lightweight functional material, magnesium plays an important role in the development of green, low-carbon and high-quality materials [1]. Magnesium and its alloys are widely used in the military, automobile industry, metallurgy, mining and other fields [2–5].

In China, the Pidgeon process, a silicothermic reduction of magnesium oxide under high temperature and vacuum, is mainly used to produce magnesium and its production accounts for 90% of the magnesium production worldwide [6]. Although the process is simple and flexible, with the strengthening of people's attention to environmental protection, the process highlights the defects of intermittent production, long cycle and large

emission [7,8]. In the Pidgeon process, the calcined dolomite is first cooled to room temperature to prepare pellets. Second, the calcined dolomite at room temperature is reheated to 1423–1523 K. This process causes a waste of energy. According to the material balance calculation, nearly 10 t of standard coal is consumed per ton of magnesium and nearly 30 t of CO_2 is discharged [9]. Under the new situation of rising prices of resources, energy and bulk raw materials, the advantage of cost performance in metal magnesium is gradually highlighted; as a consequence, the innovative development and application cases of production technology of metal magnesium are emerging, such as the aluminothermic method [10], carbothermic method [11,12], MTMP method [13], one-step method [14,15] and microwave magnesium smelting [16], which provide new ideas for industrial magnesium smelting.

In the view of the defects of high pollution,

high energy consumption and discontinuity in the process of extracting metal magnesium by the Pidgeon process, ZHANG et al [17] proposed the process of using prefabricated pellets to produce metal magnesium under flowing inert gas (rather than vacuum conditions), which was also known as magnesium smelting under relative vacuum. Some researchers [18–20] also studied the extraction of magnesium by silicothermic reduction in flowing argon and proved that it was feasible to extract metal magnesium in flowing argon, which could give the pellets a vacuum environment. In comparison to conventional technology, complete vacuum environment was not needed. The process solved the problems of intermittent production, high labor intensity, heavy pollution and low production efficiency of the current magnesium smelting method. In addition, the special calcination equipment and a vacuum system were not needed.

In the past, $\text{MgCO}_3\text{--CaCO}_3\text{--Si}$ system was deeply studied, which included the quality of prefabricated pellets, the decomposition rate of dolomite in pellets and the compressive strength of calcined pellets [21–23]. The reduction kinetics of dolomite particles in prefabricated pellets was studied by nonisothermal, argon-protected gravimetric analysis [24–26] and isothermal experiments. The apparent activation energies of the reaction were 280 and 218.75 kJ/mol respectively, which were lower than the apparent activation energy data obtained by MORSI et al [18] (306 kJ/mol) and WULANDARI et al [19] (299–322 kJ/mol) using traditional dolime for kinetic experiments. The possible reason was that CaSi_2 was formed in the calcination process of prefabricated pellets and was liquified in the reduction process, which reduced the diffusion resistance of silicon in the reduction process [27]. However, kinetic data on the reduction of MgO by CaSi_2 in prefabricated pellets have not been reported. Therefore, in this work, the kinetics of extracting metal magnesium from $\text{MgCO}_3\text{--CaCO}_3\text{--CaSi}_2$ pellets under relative vacuum system was mainly focused on, and the effects of the briquetting pressure, gas flow, temperature and duration on the reaction process were also explored. Parameters and a theoretical basis for the industrialization of continuous magnesium smelting were provided accordingly.

2 Experimental

2.1 Raw materials

The raw materials used in this experiment were magnesite (i.e. purchased from Haicheng, Liaoning Province, China) and analytical grade calcium carbonate. Magnesite and calcium carbonate were mixed according to the molar ratio of calcium to magnesium of 1:1 instead of dolomite. The chemical composition of magnesite is given in Table 1. In the experiment, the reducing agent was silicon–calcium alloy and the additive was calcium fluoride. The silicon–calcium alloy was purchased from Henan Province, China. The phase analysis of the silicon–calcium alloy through XRD is shown in Fig. 1. The results showed that the silicon–calcium alloy mainly contained CaSi_2 and Si with a small amount of SiO_2 , FeSi_2 and SiC. After chemical analysis, it could be seen that the content of CaSi_2 was 63.36%. Moreover, calcium fluoride was a chemical reagent purchased from Sinopharm Chemical Reagent Co., Ltd.

Table 1 Chemical composition of magnesite ore (wt.%)

Ignition loss	SiO_2	Al_2O_3	Fe_2O_3	CaO	MgO
51.92	0.75	0.19	0.74	0.90	45.50

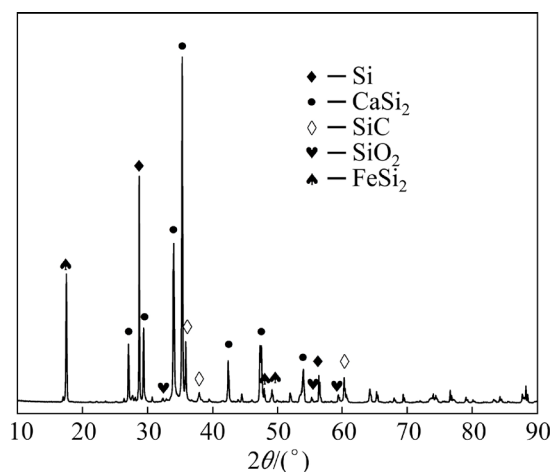


Fig. 1 XRD pattern of silicon–calcium alloy

2.2 Experimental apparatus

The experiment was carried out in a resistance furnace. The maximum furnace temperature of the resistance furnace reached 1873 K and the diameter of the furnace tube was 70 mm. The schematic diagram of the resistance furnace equipment is

shown in Fig. 2. The equipment could be vacuumized. Before the experiment, the furnace tube could be vacuumized and filled with argon to discharge the air in the furnace tube to reduce the extent of oxidation of the reducing agent and minimize the experimental error.

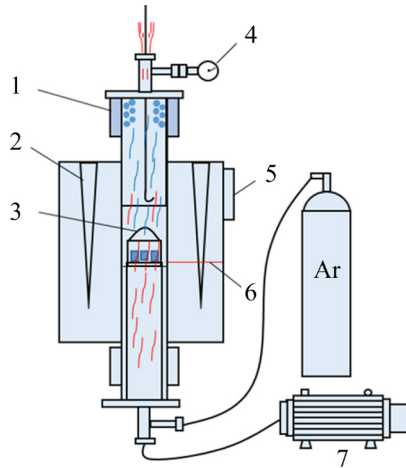
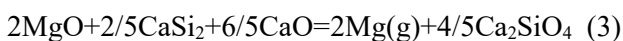


Fig. 2 Schematic diagram of equipment: 1—Water jacket; 2—Silicon-molybdenum bar; 3—Porous crucible; 4—Vacuum display instrument; 5—Control dial; 6—Thermocouple; 7—Vacuum pump

2.3 Experimental procedures

Magnesite and silicon-calcium alloy were crushed and ground to 74 μm at maximum, and then the pellets were prepared. Although magnesium oxide, calcium oxide and calcium disilicide can react with Reactions (2) and (3), Reaction (2) using CaSi_2 as reactant to generate CaSi , Mg and Ca_2SiO_4 has lower Gibbs free energy [27]. Therefore, according to the molar ratio of magnesite, calcium carbonate and calcium disilicide being 2:2:1, the reaction was expected to be as follows (Reactions (1) and (2)):



Subsequently, 3% of the total mass of calcium fluoride was added to the mixed raw material. Finally, the mixed powder was pressed into cylindrical pellets with a diameter of 15 mm by hydraulic equipment with controllable pressure. The prefabricated pellets were placed in the corundum crucible with holes and calcined in the furnace at 1273 K for 1 h. After calcination, the pellet

appearance remained intact without cracks. The XRD patterns of the products at different calcination temperatures are shown in Fig. 3. There was no Ca_2SiO_4 in the product when the pellet was calcined below 1273 K, which indicated that there was no reduction reaction in the calcination stage. After that, the crucible was lifted 25 cm away from the reaction zone and the furnace continued to be heated up. It should be emphasized that the pellets would not carry out the reduction reaction during the heating process of the furnace. After reaching the reduction temperature, the crucible was returned to the original position for the reduction experiment. The specific isothermal reduction operation method has been described in detail in the previous literature [25]. After the experiment, the phase analysis and magnesium content in the cooling slag were determined by X-ray diffraction (XRD, Bruker D8, Germany) and inductively coupled plasma emission spectrometry (ICP-OES, Optima 8300DV, Perkin-Elmer, USA), respectively. The reduction rate of magnesium was calculated by

$$\eta_{\text{Mg}} = \frac{m_1 \cdot \alpha - m_2 \cdot \beta}{m_1 \cdot \alpha} \quad (4)$$

where η_{Mg} is the reduction rate of magnesium, m_1 is the initial mass of prefabricated pellets, α is the magnesium content of the prefabricated pellets, m_2 is the mass of magnesium slag, and β is the magnesium content of magnesium slag.

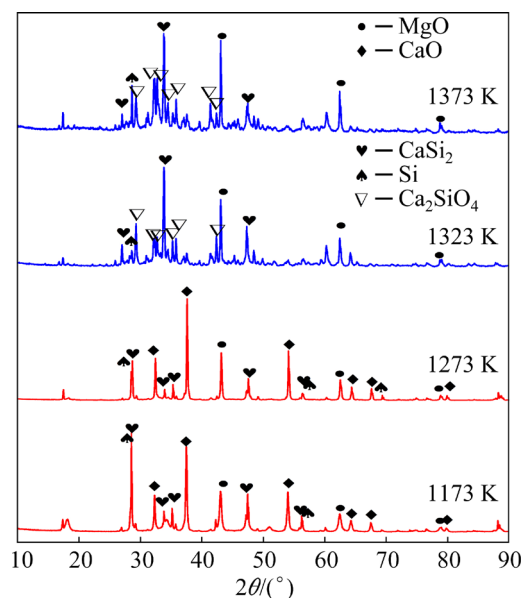


Fig. 3 XRD patterns of products calcined at different temperatures for 1 h

3 Results and discussion

3.1 Kinetic analysis

The pellets containing 15% excess calcium silicide were calcined at 1273 K for 1 h. The reduction experiments were carried out at 1423, 1473, 1523 and 1573 K. During calcination and reduction, there was argon with a flow rate of 0.2 m³/h in the furnace tube throughout the process. Figure 4(a) expresses the effects of reduction temperature and reduction time on the reduction rate.

The kinetic formula is expressed as follows:

$$\frac{dx}{dt} = k(T)f(x) \quad (5)$$

where x is the reaction degree, which is defined by

$$x = \frac{\eta_t - \eta_0}{\eta_f - \eta_0} \quad (6)$$

where η_t is the reduction ratio at time t , η_f is the final reduction ratio at the end of the experiment and η_0 is the initial reduction ratio. In the present case, $x = \eta_t$ can be obtained since $\eta_f = 1$ and $\eta_0 = 0$. Integration of Eq. (5) gives the relationship between x and t . The functions $F(x)$ are given in Table 2.

$$F(x) = \int_0^x \frac{1}{f(x)} dx = k(T)t \quad (7)$$

The function $F(x)$ in Table 2 was substituted into Eq. (6). The relationship between $F(x)$ and t at different temperatures could obtain the fitting line by using the reduction rate in Fig. 4(a). According to the fitting lines, Adj. R^2 values could be obtained.

Figure 4(c) shows the Adj. R^2 values of the fitting lines. The reduction stage can be explained by Function F_1 . According to Fig. 4(b), the values of k are determined to be 0.00041, 0.00065, 0.00085 and 0.00098 s⁻¹ at temperatures of 1423, 1473, 1523 and 1573 K, respectively, indicating that the reduction was greatly enhanced at higher temperature. In addition, the results also showed that the reduction reaction taking place on the surface of magnesium oxide particles was one of the rate controlling steps of the reduction of magnesium oxide. Consequently, the reduction stage was controlled by the chemical reaction in 1 h.

According to the fitting results, the reduction rate of metal magnesium under different conditions was calculated, and the experimental value and calculated value are compared in Fig. 4(a). It can be seen that the calculated values of reduction rate were close to the actual conversion rate of the reaction, which also showed that the selected kinetic model was appropriate.

The activation energy of this reaction was calculated by plotting $\ln k$ with $1/T$, based on the following formula:

$$k = A \exp\left(-\frac{E}{RT}\right) \quad (8)$$

where A is the preexponential constant (s⁻¹), R is the molar gas constant (J/(mol·K)) and E is the apparent activation energy (J/mol). The results are shown in Fig. 4(d). The apparent activation energy of magnesium oxide reduction by calcium silicide in a flowing argon atmosphere is 108.99 kJ/mol. The results showed that the apparent activation

Table 2 Different reaction models used to describe reduction kinetics

Symbol	$f(x)$	$F(x)$	Kinetic characteristics of reaction process
D1	$1/(2x)$	x^2	One-dimensional diffusion
D2	$[-\ln(1-x)]^{-1}$	$x+(1-x)\ln(1-x)$	Two-dimensional diffusion; cylindrical symmetry
D3	$1.5(1-x)^{2/3}[1-(1-x)^{1/3}]^{-1}$	$[1-(1-x)^{1/3}]^2$	Three-dimensional diffusion; spherical symmetry; Jander equation
D4	$1.5[(1-x)^{-1/3}-1]^{-1}$	$(1-2x/3)-(1-x)^{2/3}$	Three-dimensional diffusion; spherical symmetry; Ginstling–Brounstein equation
F1	$1-x$	$-\ln(1-x)$	First order reaction
A2	$2(1-x)[- \ln(1-x)]^{1/2}$	$[- \ln(1-x)]^{1/2}$	Random nucleation; Avrami I equation
A3	$3(1-x)[- \ln(1-x)]^{2/3}$	$[- \ln(1-x)]^{1/3}$	Random nucleation; Avrami II equation
R2	$2(1-x)^{1/2}$	$1-(1-x)^{1/2}$	Phase boundary reaction; cylindrical symmetry
R3	$3(1-x)^{2/3}$	$1-(1-x)^{1/3}$	Phase boundary reaction; spherical symmetry

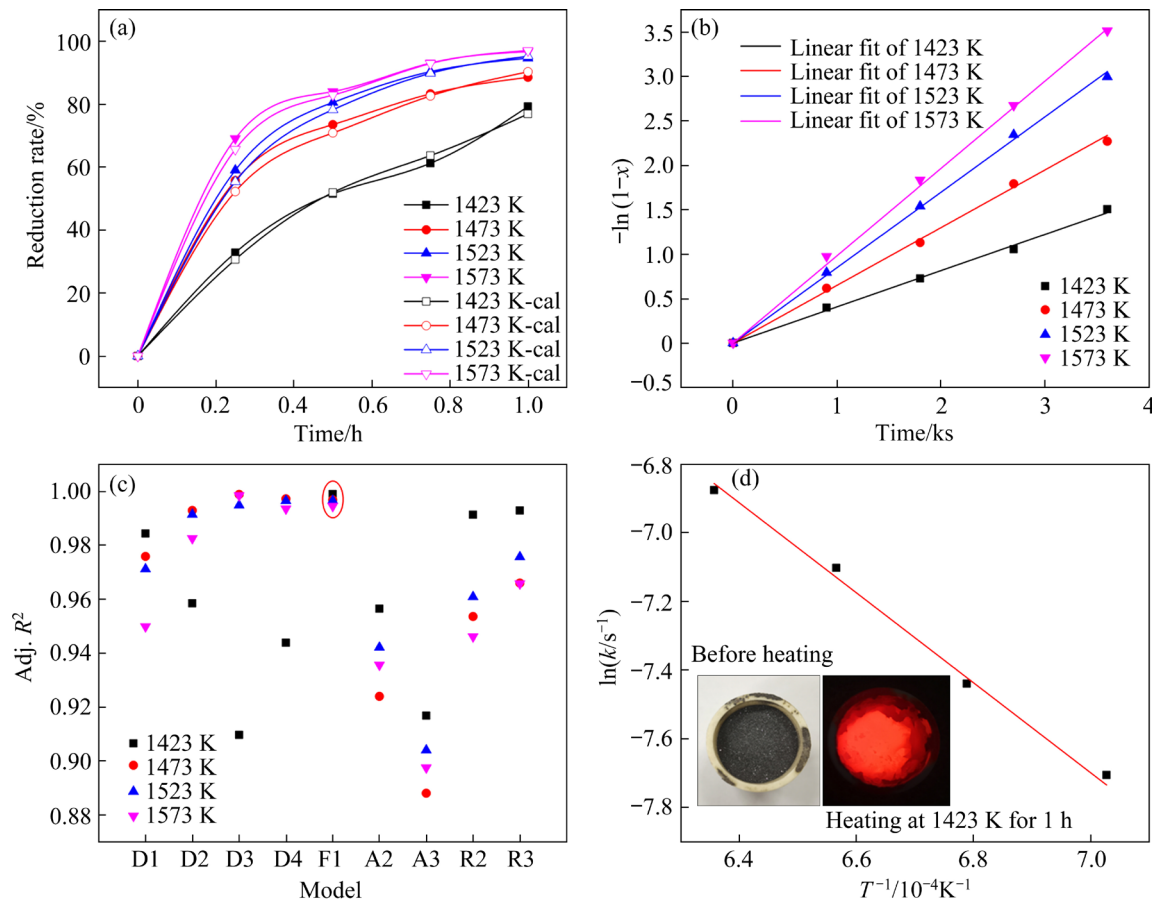


Fig. 4 Reduction rate of magnesium oxide at different time and temperatures (a); Fitting line of F₁ model at different temperatures (b); Adj. R^2 values of fitting lines (c); Relationship between $\ln k$ and $1/T$ (d)

energy of magnesium oxide reduction by calcium silicide in flowing argon atmosphere was lower than that of the traditional pellets with ferrosilicon as a reducing agent, which was between 299 and 322 kJ/mol [17,18]. The apparent activation energy was similar to that of aluminothermic reduction magnesium oxide, which was 109 kJ/mol [28]. Therefore, it could be inferred that CaSi_2 was highly similar to aluminum, and its reaction with magnesium oxide was a liquid–solid reaction, which could accelerate the reaction speed. To prove this conjecture, when CaSi_2 powder was heated at 1423 K for 1 h, CaSi_2 powder melted into liquid, as shown in Fig. 4(d).

3.2 Effect of argon flow on CaCO_3 – MgCO_3 – CaSi_2 system

Since the whole experimental process was carried out in a flowing argon atmosphere, the magnesium vapor generated on the pellet surface was carried to the condensation zone through the flowing argon, and the reaction continued to occur

by reducing the magnesium vapor partial pressure on the pellet surface. Therefore, the gas flow has a certain influence on the partial pressure of magnesium vapor. In this work, the influence of gas flow on the reaction process of magnesium oxide in the system was explored. The pellets were calcined at 1273 K for 1 h and reduced at 1573 K for 1 h with an argon flow rate from 0.1 to 0.5 m^3/h . Figure 5(a) shows the reduction rate of magnesium oxide under different argon flow rates.

When the argon flow rate was from 0.1 to 0.2 m^3/h , the reduction rate of magnesium oxide increased by 5.16% from 91.55% to 96.71%. When the gas flow rate was 0.2 m^3/h , the reduction rate reached the maximum. The trend showed that a small amount of argon flow can greatly improve the reduction rate of magnesium oxide. When the carrier gas flow increased, the partial pressure of magnesium vapor in the furnace tube decreased, and the magnesium vapor escaping from the reaction zone was not hindered; therefore, the reduction rate of magnesium oxide increased. This

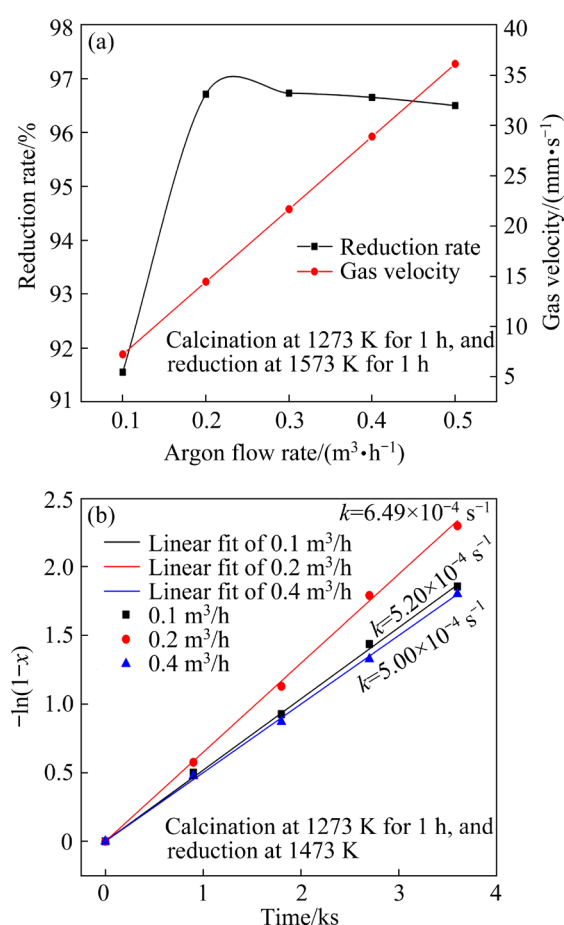


Fig. 5 Reduction rate of magnesium oxide under different argon flows (a), and apparent rate constants at different argon flow rates (b)

showed that gas film mass transfer had a certain impact on recovery of metal magnesium [24,28]. When the gas flow rate was increased from 0.2 to 0.5 m³/h, the reduction rate of magnesium oxide decreased slightly, which was inconsistent with the expected results. According to the above kinetic analysis, the reaction control step of extracting magnesium from dolomite by using CaSi₂ was a chemical reaction and the effect of temperature on the reduction rate was greater than that of gas flow. Due to the increase in the gas flow rate, preheating in the furnace tube was not sufficient to reach the temperature of the pellet placement position. When the gas flowed through the pellet surface, the pellet temperature was reduced, resulting in a low reduction rate of magnesium oxide. By fitting and calculating the reduction rates of pellets under different carrier gas flow rates, the apparent rate constants of reactions under different flow rates were obtained, as shown in Fig. 5(b). It can be seen that when the carrier gas flow was 0.1, 0.2 and

0.4 m³/h, the corresponding apparent rate constants were 5.20×10^{-4} , 6.49×10^{-4} , and $5.00 \times 10^{-4} \text{ s}^{-1}$, respectively. It can also be seen from the apparent rate constant that the effect of gas flow on the whole reduction process was consistent with the above results.

3.3 Effect of briquetting pressure on CaCO₃–MgCO₃–CaSi₂ system

The briquetting pressure of pellets directly affects density and strength of pellets. Therefore, in this work, the effect of the briquetting pressure on the reduction rate was investigated when the pressure indicators of the briquetting equipment were 5, 10, 15, 20 and 25 MPa. The actual pressure values of the briquetting equipment were 69.69, 139.38, 209.07, 278.76 and 348.45 MPa, since the diameter of the pellets was different from that of the briquetting equipment. The pellets were calcined at 1273 K for 1 h and then reduced at 1573 K for 1 h. During the experiment, the argon flow was 0.2 m³/h. The experimental results are shown in Fig. 6(a).

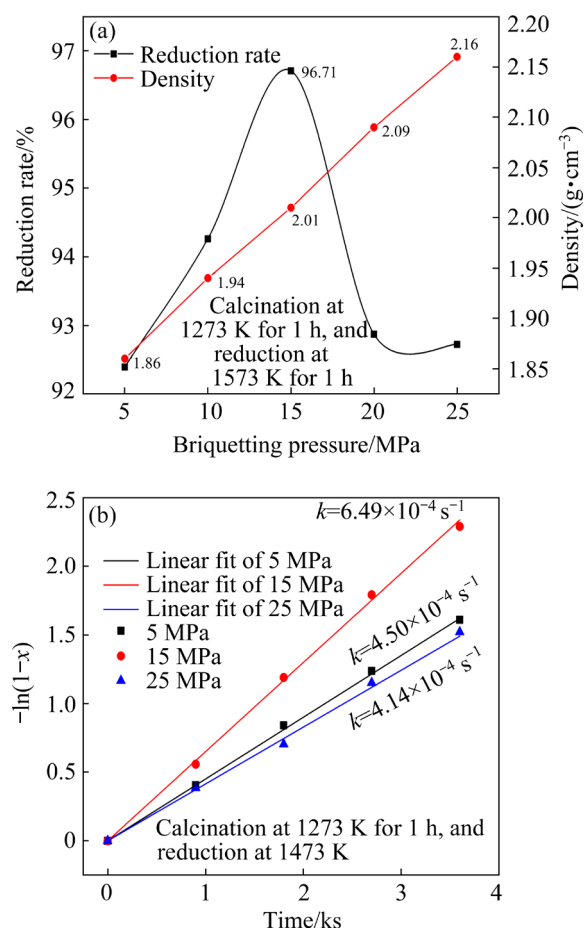


Fig. 6 Reduction rate of magnesium oxide under different briquetting pressures (a), and apparent rate constants at different briquetting pressures (b)

The results showed that the pellet density increased with increasing briquetting pressure. When the briquetting pressure was 25 MPa, the pellet density was 2.16 g/cm³. It can also be seen intuitively from Fig. 6(a) that with the increase of briquetting pressure, the reduction rate of magnesium oxide first increased, and then decreased. When the briquetting pressure was 15 MPa, the reduction rate of magnesium oxide was the maximum at 96.71%. This was because increasing the briquetting pressure enlarged the contact area between magnesium oxide and CaSi₂, which improved the penetration of molten CaSi₂ into the magnesium oxide phase and the reduction of magnesium oxide. However, if the briquetting pressure was too high, the molten CaSi₂ and reaction products would prevent the diffusion of metal magnesium vapor and reduce the recovery of metal magnesium, thus affecting the reduction rate of magnesium oxide. By calculating the reduction rates of pellets under different briquetting pressures and performing regression analysis at 1473 K, the apparent rate constants of pellets under different briquetting pressures were obtained, as shown in Fig. 6(b). When the briquetting pressure was 5, 15 and 25 MPa, the apparent rate constants were 4.50×10^{-4} , 6.49×10^{-4} and $4.14 \times 10^{-4} \text{ s}^{-1}$, respectively. The reaction rate was again larger when the pelletizing pressure was 15 MPa. This experimental phenomenon also showed that the appropriate briquetting pressure was also very important to obtain a higher reduction rate of magnesium oxide.

3.4 Effect of temperature and time on CaCO₃–MgCO₃–CaSi₂ system

The reduction rate of magnesium oxide of prefabricated pellets with CaSi₂ as a reducing agent was investigated in the temperature range of 1423–1573 K for 0–4 h. Since the crucible for placing pellets was placed in the reaction zone after the furnace temperature reached the set temperature, the reduction rate of pellets was zero at the start.

The experimental results shown in Fig. 7 indicated that the reduction rate of magnesium oxide changed rapidly within 45 min at different temperatures. The corresponding reduction rates at 45 min from 1423 to 1573 K were 61.27%, 83.35%, 90.41% and 93.11%, respectively. The reduction rate increased by 22.08% from 1423 to 1473 K, 7.06% from 1473 to 1523 K and 2.7% from 1523 to

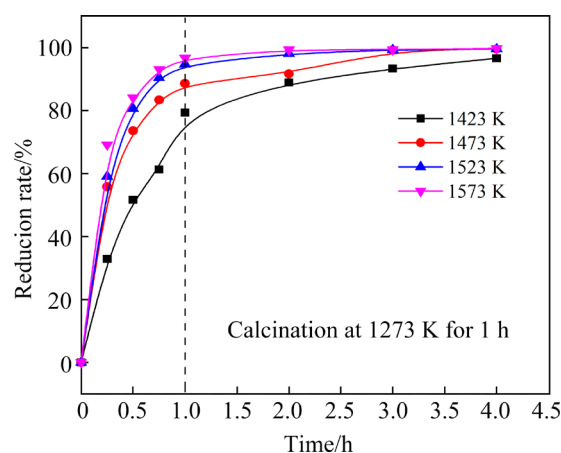


Fig. 7 Reduction rate of magnesium oxide at different temperatures and time

1573 K. At 1473, 1523 and 1573 K, the reduction rates of magnesium oxide were 36.96%, 58.4% and 65.06%, respectively, with ferrosilicon as the reducing agent at the same reduction time, which was obviously lower than the reduction rate of magnesium oxide when CaSi₂ was used as the reducing agent [25]. With the elevation in temperature, the increase rate of reduction slowed down. This was because the reaction rate was larger at high temperature. Meanwhile, for pellets at higher temperatures, the reaction was closer to the reaction end point and the reaction rate became less; therefore, the increasing rate of reduction slowed down. At the same temperature, from 1 to 4 h, the reduction rate of magnesium oxide increased by 17.28%, 10.97%, 4.92% and 3.03% at 1423, 1473, 1523 and 1573 K, respectively. This was because the chemical reaction is the rate determining step rather than diffusion. At high temperature, the reaction rate was larger in the early stage of the reaction, which consumed a large amount of reducing agent, resulting in less available reducing agent, less reaction rate and the slowdown in the increasing rate of reduction in the later stage of the reaction.

According to the above results, XRD analysis was carried out on the reduction slag with different reduction time at 1473 K. The results shown in Fig. 8 suggested that the slag contained CaO, MgO, CaSi₂ and Ca₂SiO₄ after reduction for 15 min. In addition, it could be found that with the extension of reduction time, the MgO peak decreased gradually. After 120 min, the intensity of the MgO peak was very low, indicating that the reduction

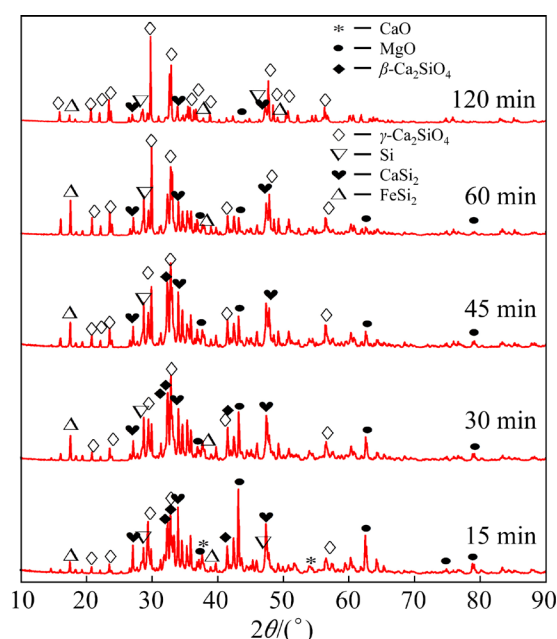


Fig. 8 XRD patterns of magnesium slag with different reduction time at 1473 K

was complete. According to XRD analysis, no CaSi phase was found in the product, which was probably due to the instability of CaSi. Under the experimental conditions, CaSi was re-decomposed into Ca and CaSi₂ to participate in the reduction reaction of magnesium oxide. According to the data [29], in a liquid phase CaSi alloy, the vapor pressure of Ca could reach 13 Pa at 1423 K and was higher with the increase of temperature. Therefore, the generated Ca vapor was sufficient to reduce MgO. Compared with ferrosilicon, this could also be one of the reasons why CaSi₂ had a larger reduction rate in reducing MgO.

According to the XRD standard diffraction peak of dicalcium silicate, the 2θ values of the strongest peak and secondary peak of β -Ca₂SiO₄ are 32.156° and 32.762°, respectively, while those of the strongest peak and secondary peak of γ -Ca₂SiO₄ are 32.788° and 29.635°, respectively, so it can be distinguished by the secondary peak and other peaks in the β and γ phases. Figure 8 shows that with the extension of reduction time, β -Ca₂SiO₄ gradually disappeared and transformed into γ -Ca₂SiO₄. After reduction for 120 min, there was only the γ -Ca₂SiO₄ phase in the reduction slag, and the MgO content in the reduction slag was 2.03%.

Previous studies [30–32] have shown that, foreign ions can cause dicalcium silicate to present different crystal types. The solid solution of foreign

ions into the dicalcium silicate crystal could prevent the transformation of the high-temperature crystal type to the low-temperature crystal type in the process of temperature drop, thus stabilizing β -Ca₂SiO₄ to room temperature. It was speculated that the reason could be that a certain amount of MgO had a stabilizing effect on β -Ca₂SiO₄. With the decrease of MgO content in slag, less than 2.03%, MgO lost its stabilizing effect on β -Ca₂SiO₄. Eventually, β -Ca₂SiO₄ was transformed into γ -Ca₂SiO₄. Figure 9 shows SEM images and EDS results of magnesium slag after reduction at 1473 K for different time. It can be seen from the figure that when reducing for 15 min, a large amount of MgO was attached to Ca₂SiO₄ and the reduction was not complete. With the increase of reduction time, the MgO content gradually decreased and the surface of Ca₂SiO₄ was smooth, lamellar and well-crystallized.

According to the method in Refs. [18,19], the actual magnesium vapor pressure difference between the pellet surface and argon was calculated. It is assumed that the magnesium vapor diffuses into the gas and mixes uniformly with the inert gas. The mass transfer process of magnesium vapor can be expressed as follows:

$$j = \frac{M}{RT} k_c (P_B - P_S) \quad (9)$$

Equation (9) can be arranged into

$$\Delta P = \frac{RT}{Mk_c} \frac{N}{S} \quad (10)$$

where j is the magnesium mass transfer flux, g/(cm²·s), M is the atomic mass of magnesium, 24.3 g/mol, P_B and P_S are magnesium partial pressures in the inert gas and on the pellet surface, respectively, Pa, N is the generation rate of magnesium, g/s, S is the pellet surface area, m², k_c is the mass transfer coefficient, and $\Delta P = P_B - P_S$.

Since the gas stream passes through an annulus formed by the cylindrical pellet and crucible, k_c can be calculated.

According to Eqs. (9) and (10), the mass transfer coefficients of magnesium vapor in flowing argon at temperatures between 1423 and 1573 K can be obtained. When the argon flow was 0.2 m³/h, mass transfer coefficients at different temperatures were 0.054, 0.057, 0.060 and 0.063 m/s, respectively. Based on the mass transfer coefficient, the difference between the magnesium partial pressure

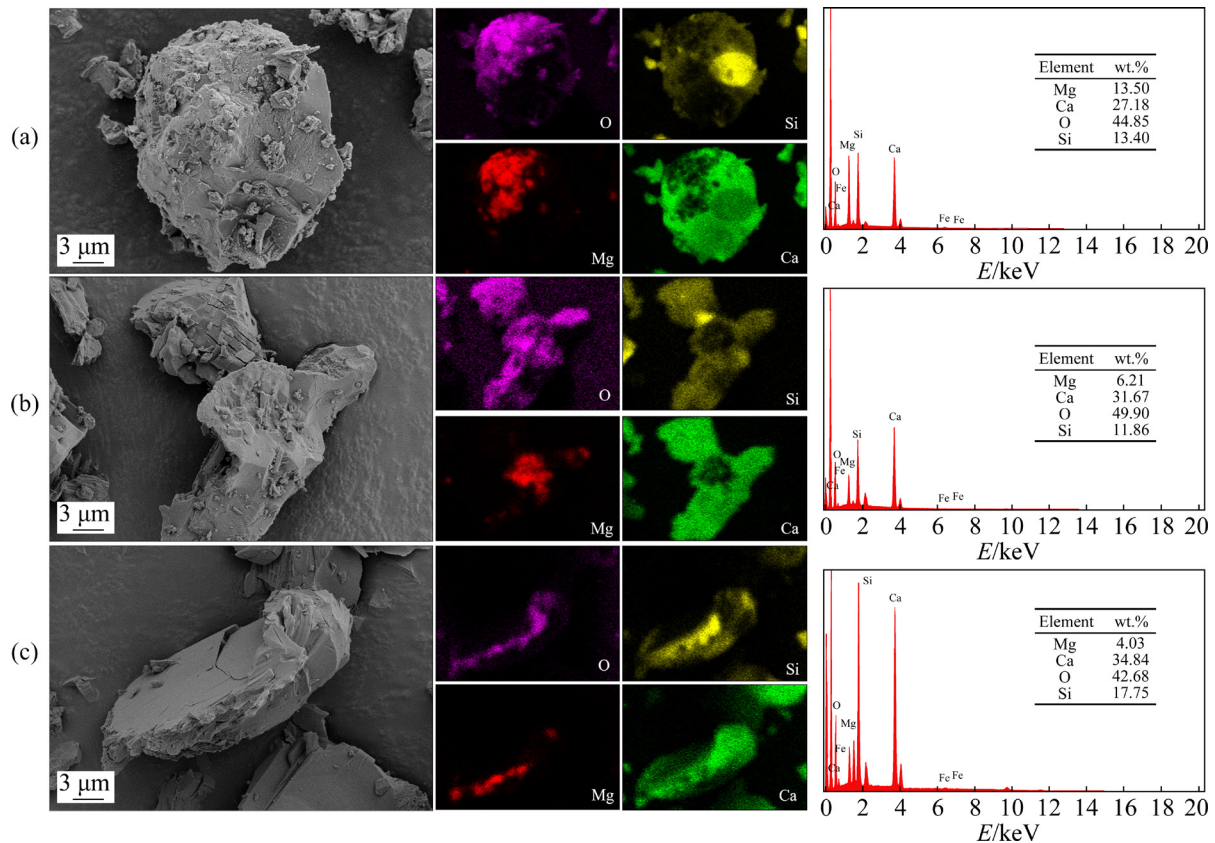


Fig. 9 SEM images and EDS result of magnesium slag after reduction at 1473 K for different time: (a) 15 min; (b) 60 min; (c) 120 min

on the pellet surface in flowing argon and the partial pressure in argon gas flow could be estimated, as shown in Fig. 10.

Due to the continuous flow of argon, the argon near the pellets was constantly updated and the magnesium partial pressure in argon was negligible compared with the magnesium partial pressure on the pellet surface. Therefore, the magnesium partial pressure in argon near the pellets could be considered to be zero, and ΔP was the actual magnesium partial pressure on the pellets surface. It can be seen that the higher the temperature is, the greater the partial pressure on the pellet surface, indicating that the reaction was violent. When the reduction time was 0.25 h at 1573 K, the partial pressure on the pellet surface was 5.35 kPa. With the extension of reaction time, the partial pressure of magnesium vapor continuously decreased to 0.519 kPa at 4 h. Figure 10 also shows that the magnesium partial pressure on the pellet surface decreased with decreasing temperature. When the reduction temperature was 1423 K and reduction time was 0.25 h, the partial pressure of magnesium

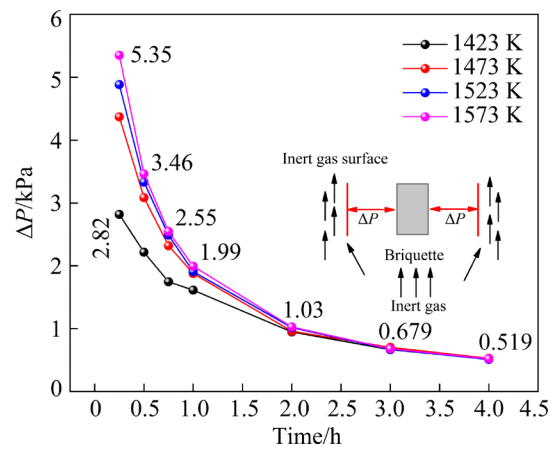


Fig. 10 Calculated differential pressure (ΔP) of magnesium vapor on surface of briquette and bulk phase at 1423–1573 K

on the pellet surface was 2.82 kPa. Compared with 1573 K, the partial pressure of magnesium on the pellet surface was reduced by nearly 50%, which indicated that the temperature had a great influence on the reduction reaction, which also reflected that the reaction could be controlled by chemical reaction.

4 Conclusions

(1) The reduction process of magnesium oxide by CaSi_2 was a solid–liquid reaction. The process of extracting magnesium from prefabricated pellets in flowing argon can be explained by Model F_1 . This process was controlled by chemical reactions instead of diffusion. The apparent activation energy was 108.99 kJ/mol.

(2) A small argon flow rate could greatly improve the reduction rate of magnesium oxide and gas film mass transfer had a certain impact on the recovery of magnesium. In addition, the appropriate briquetting pressure could obtain better recovery of magnesium.

(3) As a reducing agent, CaSi_2 had a large reduction rate of magnesium oxide. The reaction process was close to the end point after reduction for 1 h. The content of MgO in the reduction slag could affect the crystal form of Ca_2SiO_4 .

Acknowledgments

This work was supported by the National Natural Science Foundation of China (Nos. U1508217, 51504058), and the Fundamental Research Funds for the Central Universities of China (No. N162504003).

References

- [1] HIRSCH J, Al-SAMMAN T. Superior light metals by texture engineering: Optimized aluminum and magnesium alloys for automotive applications [J]. *Acta Materialia*, 2013, 61(3): 818–843. DOI: 10.1016/j.actamat.2012.10.044.
- [2] HANKO G, AHREKOWITSCH H, EBNER P. Recycling automotive magnesium scrap [J]. *JOM*, 2002, 54(2): 51–54. DOI: 10.1007/BF02701075.
- [3] JOOST W J, KRAJEWSKI P E. Towards magnesium alloys for high-volume automotive applications [J]. *Scripta Materialia*, 2017, 128: 107–112. DOI: 10.1016/j.scriptamat.2016.07.035.
- [4] KUMAR A, KUMAR S, MUKHOPADHYAY N K. Introduction to magnesium alloy processing technology and development of low-cost stir casting process for magnesium alloy and its composites [J]. *Journal of Magnesium and Alloys*, 2018, 6(3): 245–254. DOI: 10.1016/j.jma.2018.05.006.
- [5] KULEKCI M K. Magnesium and its alloys applications in automotive industry [J]. *The International Journal of Advanced Manufacturing Technology*, 2008, 39: 851–865. DOI: 10.1007/s00170-007-1279-2.
- [6] HAN Ji-biao, FU Da-xue, GUO Jun-hua, ZHANG Ting-an. Nucleation and condensation of magnesium vapor in argon carrier [J]. *Metals*, 2020, 10(11): 1441. DOI: 10.3390/met10111441.
- [7] GAO Feng, NIE Zuo-ren, WANG Zhi-hong, GONG Xian-zheng, ZUO Tie-yong. Assessing environmental impact of magnesium production using Pidgeon process in China [J]. *Transactions of Nonferrous Metals Society of China*, 2008, 18(3): 749–754. DOI: 10.1016/S1003-6326(08)60129-6.
- [8] DU Jin-dan, HAN Wei-jian, PENG Ying-hong. Life cycle greenhouse gases, energy and cost assessment of automobiles using magnesium from Chinese Pidgeon process [J]. *Journal of Cleaner Production*, 2010, 18(2): 112–119. DOI: 10.1016/j.jclepro.2009.08.013.
- [9] RAMAKRISHNAN S, KOLTUN P. Global warming impact of the magnesium produced in China using the Pidgeon process [J]. *Resources, Conservation and Recycling*, 2004, 42(1): 49–64. DOI: 10.1016/j.resconrec.2004.02.003.
- [10] FU Da-xue, FENG Nai-xiang, WANG Yao-wu, PENG Jian-ping, DI Yue-zhong. Kinetics of extracting magnesium from mixture of calcined magnesite and calcined dolomite by vacuum aluminothermic reduction [J]. *Transactions of Nonferrous Metals Society of China*, 2014, 24(3): 839–847. DOI: 10.1016/S1003-6326(14)63133-2.
- [11] TIAN Yang, XU Bao-qiang, YANG Bin, YANG Cheng-bo, QU Tao, LIU Da-chun, DAI Yong-nian. Magnesium production by carbothermic reduction in vacuum [J]. *Journal of Magnesium and Alloys*, 2015, 3: 149–154. DOI: 10.1016/j.jma.2015.04.001.
- [12] YANG Cheng-bo, TIAN Yang, QU Tao, YANG Bin, XU Bao-qiang, DAI Yong-nian. Magnesium vapor nucleation in phase transitions and condensation under vacuum conditions [J]. *Transactions of Nonferrous Metals Society of China*, 2014, 24(2): 561–569. DOI: 10.1016/S1003-6326(14)63096-X.
- [13] ABDELLATIF M. Review of the development work on the Mintek thermal magnesium process (MTMP) [J]. *Journal South African Institute Mining Metallurgy*, 2011, 111: 393–399.
- [14] ZHANG Chao, WANG Chao, ZHANG Shao-Jun, GUO Lie-jie. Experimental and numerical studies on a one-step method for the production of Mg in the silicothermic reduction process [J]. *Industrial & Engineering Chemistry Research*, 2015, 54: 8883–8892. DOI: 10.1021/acs.iecr.5b01830.
- [15] ZHANG Chao, WANG Chao, ZHANG Shao-Jun, GUO Lie-jie. The effects of hydration activity of calcined dolomite (HCD) on the silicothermic reduction process [J]. *International Journal of Mineral Processing*, 2015, 142: 154–160. DOI: 10.1016/j.minpro.2015.01.008.
- [16] WADA Y, FUJII S, SUZUKI E, MAITANI M M, TSUBAKI S, CHONAN S, FUKUI M, INAZU N. Smelting magnesium metal using a microwave Pidgeon method [J]. *Scientific Reports*, 2017, 7(1): 46512. DOI: 10.1038/srep46512.
- [17] ZHANG Ting-an, DOU Zhi-he, ZHANG Zi-mu, LIU Yan, LV Guo-zhi, HE Ji-cheng. A method of rapid continuous extraction of magnesium: China Patent, CN 104120282 A [P]. 2014–10–29.
- [18] MORSI I M, EIBARAWY K A, MORSI M B, ABDEL-GAWAD S R. Silicothermic reduction of dolomite ore under

- inert atmosphere [J]. Canadian Metallurgical Quarterly, 2002, 41(1): 15–28. DOI: 10.1179/cmqr.2002.41.1.15.
- [19] WULANDARI W, BROOKS G A, RHAMDHANI M A, MONAGHAN B J. Kinetic analysis of silicothermic process under flowing argon atmosphere [J]. Canadian Metallurgical Quarterly, 2014, 53(1): 17–25. DOI: 10.1179/1879139513Y.0000000096.
- [20] BARUA S K, WYNNYCKYI J R. Kinetics of the silicothermic reduction of calcined dolomite in flowing hydrogen [J]. Canadian Metallurgical Quarterly, 1981, 20(3): 295–306. DOI: 10.1179/cmqr.1981.20.3.295.
- [21] WAN Ming, ZHANG Ting-an, DOU Zhi-he, ZHOU Lian. Pellets preparation by direct briquetting for silicothermic magnesium production [J]. Journal of Northeastern University (Natural Science), 2014, 35(10): 1460–1463. (in Chinese). DOI: 10.3969/j.issn.1005-3026.2014.10.021.
- [22] WEN Ming, ZHANG Ting-an, DOU Zhi-he, GUAN Yue, ZHANG Rui. Two-stage calcination of dolomite pellets for mg-extraction by silicothermic reduction in vacuum [J]. Chinese Journal of Vacuum Science and Technology, 2014, 34(11): 1242–1245. (in Chinese). DOI: 10.13922/j.cnki.cjovst.2014.11.19.
- [23] GUO Jun-hua, ZHANG Ting-an, FU Da-xue, HAN Ji-biao, DOU Zhi-he. Research on properties of prefabricated pellets of silicothermic process after calcination in flowing argon atmosphere [C]//Magnesium Technology 2020. San Diego, PA: TMS, 2020: 303–307. DOI: 10.1007/978-3-030-36647-6-45.
- [24] FU Da-xue, ZHANG Ting-an, GUAN Lu-kui, DOU Zhi-he, WEN Ming. Magnesium production by silicothermic reduction of dolime in pre-prepared dolomite pellets [J]. JOM, 2016, 68: 3208–3213. DOI: 10.1007/s11837-016-2034-7.
- [25] GUO Jun-hua, FU Da-xue, HAN Ji-biao, JI Zong-hui, DOU Zhi-he, ZHANG Ting-an. Kinetics of extracting magnesium from prefabricated pellets by silicothermic process under flowing argon atmosphere [J]. Journal of Mining and Metallurgy Section B–Metallurgy, 2020, 56(3): 379–386. DOI: 10.2298/JMMB200712031G.
- [26] CHE Yu-si, MAI Geng-peng, ZHANG Shao-jun, HE Ji-lin, SONG Jian-xun, YI Jian-hong. Kinetic mechanism of magnesium production by silicothermic reduction of CaO·MgO in vacuum [J]. Transactions of Nonferrous Metals Society of China, 2020, 30(10): 2812–2822. DOI: 10.1016/S1003-6326(20)65423-1.
- [27] FU Da-xue, JI Zong-hui, GUO Jun-hua, HAN Ji-biao, DOU Zhi-he, LIU Yan, ZHANG Ting-an. Diffusion and phase transformations during the reaction between ferrosilicon and CaO·MgO under vacuum [J]. Journal of Materials Research and Technology, 2020, 9(3): 4379–4385. DOI: 10.1016/j.jmrt.2020.02.062.
- [28] YANG Jian, KUWABARA M, SAWADA T, SANO M. Kinetics of isothermal reduction of MgO with Al [J]. ISIJ International, 2006, 46(8): 1130–1136. DOI: 10.2355/isijinternational.46.1130.
- [29] WYNNYCKYJ J R, PIDGEON L M. Equilibria in the silicothermic reduction of calcined dolomite [J]. Metallurgical Transactions, 1971, 2(4): 979–986. DOI: 10.1007/BF02664228.
- [30] PRITTS I M, DAUGHERTY K E. The effect of stabilizing agents on the hydration rate of β -C₂S [J]. Cement and Concrete Research, 1976, 6(6): 783–795. DOI: 10.1016/0008-8846(76)90008-9.
- [31] ISHIDA H, MABUCHI K, SASAKI K, MITSUDA T. Low-temperature synthesis of β -Ca₂SiO₄ from hillebrandite [J]. Journal of the American Ceramic Society, 1992, 75(9): 2427–2432. DOI: 10.1111/j.1151-2916.1992.tb05595.x.
- [32] GUO Jun-hua, FU Da-xue, HAN Ji-biao, JI Zong-hui, WANG Yao-song, ZHANG Ting-an. The effect of calcium fluoride on extracting magnesium from magnesite and calcium carbonate by silicothermal reduction in flowing argon [J]. Journal of Mining and Metallurgy Section B–Metallurgy, 2022, 58(1): 19–28. DOI: 10.2298/JMMB210318045G.

在相对真空下含 CaSi₂ 的预制球团还原提镁动力学

郭军华, 张延安, 韩继标, 王耀松

东北大学 冶金学院 多金属共生矿生态冶金教育部重点实验室, 沈阳 110819

摘要: 在相对真空下以 CaSi₂ 为还原剂进行预制球团提镁过程的研究。利用扫描电子显微镜(SEM)、能谱仪(EDS)和 X 射线衍射仪(XRD)分别对还原渣的形貌、化学成分和物相进行分析。结果表明, 小的氩气流量可以极大地提高氧化镁的还原率, 在相对真空下以 CaSi₂ 为还原剂的预制球团提镁过程可以用 F₁ 模型解释, CaSi₂ 还原氧化镁为固液反应, 此过程为化学反应控制, 温度对还原率影响很大, 表观活化能为 108.99 kJ/mol。还原渣的物相分析表明, 渣中的 MgO 含量对 Ca₂SiO₄ 的晶型转变有影响。

关键词: 等温动力学; 镁; 硅酸钙; 流动氩气; 硅热法

(Edited by Bing YANG)